Giant bulk photovoltaic effect and spontaneous polarization of single-layer monochalcogenides

Tonatiuh Rangel,[1,2,*] Benjamin M. Fregoso,[2,*] Bernardo S. Mendoza,[3]
Takahiro Morimoto,[2] Joel E. Moore,[2] and Jeffrey B. Neaton[1,2,4]

[1] *Molecular Foundry, Lawrence Berkeley National Laboratory, Berkeley, California 94720, USA*
[2] *Department of Physics, University of California, Berkeley, California 94720, USA*
[3] *Centro de Investigaciones en Óptica, León, Guanajuato, México*
[4] *Kavli Energy Nanosciences Institute at Berkeley, Berkeley, California 94720, USA*

We use a first-principles density functional theory approach to calculate the shift current of uniformly illuminated single-layer Ge and Sn monochalcogenides. We find a larger effective three-dimensional shift current ($\sim$ 200 μA/V^2) than has been previously observed in common polar systems. The integral of the shift-current tensor along the polarization axis, a physically relevant quantity in applications, is correlated to the large spontaneous effective three-dimensional electric polarization ($\sim$ 1.9 C/m^2), and is well described by the one-dimensional Rice-Mele tight-binding model. Using our model, we discuss the conditions under which the response is optimized as a function of the system polarization. Importantly, our calculations indicate that the shift current will be largest in the visible spectrum, suggesting these materials may be promising for polar optoelectronic devices.

Introduction: The shift current is a dc current generated in a material under uniform illumination [1–4]. It is one that gives rise to such phenomena as the bulk photovoltaic effect (BPVE) [1]. A necessary condition for the BPVE in a material is the lack of inversion symmetry. Interestingly, in the BPVE, the resulting photovoltage is not limited by the band gap energy. In addition, a junction or interface is not required to generate a current. These characteristics of the BPVE motivate great interest in possible optoelectronic applications of noncentrosymmetric systems, and they have been suggested to play a role in emerging functional materials, including hybrid halide perovskites [5].

The BPVE is much less studied in two-dimensional (2D) materials [6, 7], despite the fact that such systems represent the ultimate scaling in thickness with mechanical, optical and electronic properties unique relative to their bulk counterparts. For example, single-layer group-IV monochalcogenides GeS, GeSe, SnS and SnSe are actively being investigated [8–10] due to their promising band gaps in the UV range suitable for solar-cell applications. Centrosymmetric in the bulk, the monochalcogenides lack inversion symmetry in single-layer form, allowing for the emergence of a spontaneous polarization and a BPVE. Although inversion symmetry is necessary for a non-zero shift-current, a polarization is not required, and the relationship between polarization and shift current has not been fully elucidated [5, 11].

In this Letter we use first principles density functional theory methods, supplemented by a tight-binding model, to predict and understand the BVPE in single-layered monochalcogenides and its spontaneous electric polarization. In addition to their established favorable band gaps and strong absorption [12, 13], we demonstrate that the monochalcogenides exhibit a giant in-plane shift current, up to 200 mA/V^2. Using a Rice-Mele tight-binding model, we find that the integral of the frequency-dependent shift-current tensor is well correlated to the spontaneous polarization; this integral is maximized at an optimal value of polarization.

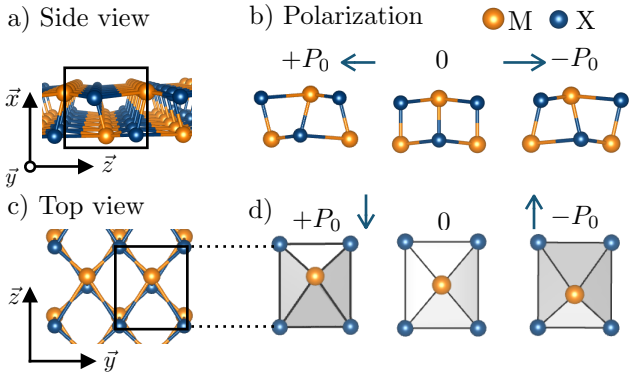

FIG. 1. (Color online) The crystal structure of single-layer group-IV monochalcogenides MX, where M=Ge,Sn, and X=S, Se. In (a) we show the 3D view of the single-layer and in (b)-(d) the projections of the single-layer crystal on the Cartesian axes. Structures with $0, \pm P$ polarizations are also shown in inset (b) and (d). A two-fold rotation along z (plus translations) determines the polarization axis, as discussed in the text. Note that there is a continuous path between configurations with various polarizations.

Structure, symmetries and ab-initio methods. Our DFT calculations are performed with the generalized gradient approximation. We use the ABINIT[14] code, with Gaussian pseudopotentials [15] and the Perdew-Burke-Ernzerhof (PBE) functional [16]. We fully relax atomic positions in supercells that include at least 10 Å of vacuum between single-layers. Our relaxed lattice parameters are shown in Table I and agree with previous work [8]

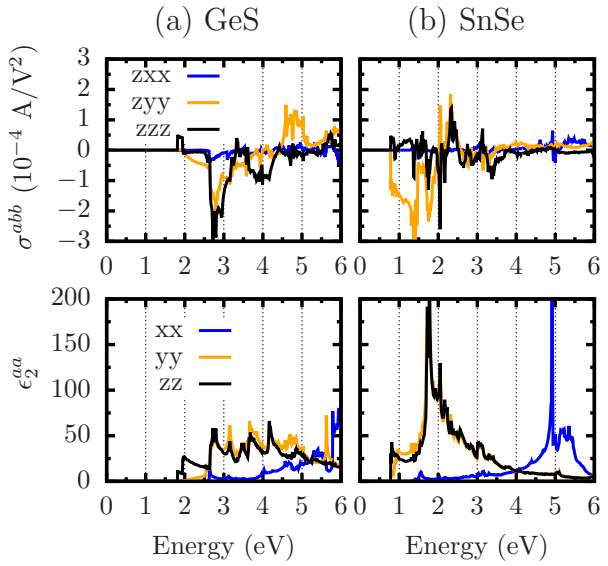

FIG. 2. (Color online) Shift-current (top panels) and absorption (bottom panels) spectrum of single-layer GeS and SnSe. There is a large in-plane shift-current response the visible frequency regime. The absorption spectra (density of states) is correlated with the *zzz* and *zyy* shift-current responses.

(see SI for details).

Bulk monochalcogenide crystals MX (M=Ge,Sn and X=S,Se) are orthorhombic with point group *mmm* and space group *Pnma* (No. 62). They consists of van der Waals-bonded double layers of metal monochalchogenide atoms in an armchair arrangement. The space group of the bulk crystal contains eight symmetries including a center of inversion which prevents spontaneous electric polarization and BPVE. Upon exfoliation, the resulting single "double layer" primitive cell has four atoms. In this work, the layers are chosen to be oriented perpendicular to the x axis as shown in Fig. 1a. The single-layer structure has four symmetries, including a two-fold rotation with respect to z (plus translations), $2[001] + (1/2, 0, 1/2)$, which determines the direction of the in-plane spontaneous polarization of the single-layer along the z axis. In addition, the 2D-system has two mirror symmetries with respect to x and y, $m[100]+(1/2, 1/2, 1/2)$ and $m[010]+(0, 1/2, 0)$. Hence its point group, which determines the non-zero components of the optical response tensors, is $mm2$.

As a consequence of the mirror symmetries with respect to the x and y axis of a single-layer, all the cross-components terms of the imaginary part of the dielectric function, ϵ_2^{ab}, vanish together with the tensor components xxx, xyy, xzz, yxx, yyy, yzz of the shift current. Only seven components are symmetry-allowed [17]: zxx, zyy, zzz, yyz and xzx, as well as components obtained by interchanging the last two indices. Symmetry, however, does not indicate the strength of the response in each direction, and consequently we must compute the matrix elements involved.

Spontaneous polarization. We calculate the spontaneous polarization of the single-layer, using the modern theory of polarization [18, 19], as implemented in ABINIT. We first identify an adiabatic path between the ground state and a centrosymmetric geometry with, in this case, zero polarization. We parametrize the atomic displacements along a path between these geometries (Fig. 1b, 1d) with λ as $\mathbf{R}^i(\lambda) = \mathbf{R}_0^i + \lambda(\mathbf{R}_f^i - \mathbf{R}_0^i)$, where $\mathbf{R}_0^i$ ($\mathbf{R}_f^i$) is the initial (final) position of ith atom in the centrosymmetric (non-centrosymmetric) structure. The polarization for various monochalcogenides has also been theoretically studied recently [20–25]. Our adiabatic polarization path, as shown schematically in Fig. 1b and (d), is similar to the one used in Refs. [24, 25].

Table I shows the spontaneous electric polarization per unit area, $P_0 a$, and an effective 3D polarization assuming an active single-layer thickness a = 2.6 Å, following recent studies [24, 25]. Interestingly, GeSe has a higher effective 3D polarization, 1.9 C/m^2, than prototypical ferroelectric systems, e.g., compare 0.0028 C/m^2 in $CaMn_7O_{12}$ [26], 0.26 C/m^2 in $BaTiO_3$ [27, 28], 0.37 C/m^2 in $KNbO_3$ [29] and 0.9 C/m^2 in $BiFeO_3$ [30, 31]. We calculate the minimum-energy path between the $\pm P_0$ configurations in the, as detailed in the SI. The minimal energy path is indistinguishable from the linear path used here. The energy barriers, provided in Table I, are much larger than room temperature. However, since reorientation is often facilitated by domain wall motion, future experiments are necessary to conclusively demonstrate ferroelectric switching behavior.

Optical absorption and shift current. One attractive feature of single-layer monochalcogenides are their promising band gaps energies in the visible range [10, 12, 13]. In Table I, we show the computed DFT-PBE gaps, which are a good estimate of the corresponding optical gaps. We expect the PBE single-particle gaps to be indicative in this case since excitonic effects, as large as 1 eV in GeS [13], can fortuitously mitigate the well-known tendency of PBE to underestimate the band gap. From the Kohn-Sham states we also calculate the imaginary part of the the dielectric function,

$$\epsilon_2^{ab}(\omega) = \delta_{ab} - \frac{e^2\pi}{\epsilon_0\hbar}\int \frac{d\mathbf{k}}{(2\pi)^3}\sum_{nm} f_{nm} r^a_{nm} r^b_{mn} \delta(\omega_{mn} - \omega), \quad (1)$$

which provides a RPA frequency dependent optical absorption spectrum. Here $r^a_{nm} = A^a_{nm} = i\langle u_n|\nabla^a|u_m\rangle$ ($n \neq m$) are the dipole matrix elements and A^a_{nm} the usual Berry connections, with the a and b indices indicating one of the three Cartesian directions. We define the occupations numbers $f_{nm} = f_n - f_m$, and the band energy differences as $\hbar\omega_{nm} = \hbar\omega_n - \hbar\omega_m$. Here and in what follows we assume zero temperature. As can be seen in Fig. 2, the absorption is strong, ~ 50, in the visible

	Polarization		Energy	Supercell			Band gap (eV)			
	2D	3D	barrier	param. (Å)			DFT-PBE		*GW*-BSE	Expt.*
	(nC/m)	(C/m^2)	(K)	a	b	c	D	I	D	D
GeS	0.48	1.9	5563	15.0	3.7	4.5	1.9	1.7	2.2 [13]	1.6 [10]
GeSe	0.34	1.3	1180	15.0	4.0	4.3	1.2	1.2	1.6, 1.3 [12, 13]	1.2 [10]
SnS	0.24	0.8	384	15.0	4.1	4.3	1.5	1.4		
SnSe	0.17	0.6	80	15.0	4.3	4.4	0.9	0.9	1.4 [12]	

TABLE I. Left: Large ground state polarization of single-layer monochalcogenides. The three-dimensional effective polarizations are computed assuming a layer thickness of $a = 2.6$ Å). The energy barrier between the ground-states with opposite polarization and supercell lattice parameters calculated with DFT-PBE are also shown. Right: Direct (D) and indirect (I) band gaps calculated with DFT-PBE and optical gaps reported from *GW*-BSE calculations. * Experimental optical gaps of few-layer chalcogenides are also shown for comparison.

range of 1.5 to 3 eV, where the zz and yy tensor components are larger than xx due to the intrinsic crystal anisotropy, in agreement with previous work [10, 12, 13]. In addition to the energy gaps and the large absorption in the visible, single-layer monochalcogenides have a large shift-current response, as we show below.

The dc shift current is generated to second order in the electric field. Consider a monochromatic electric field of the form $E^b(t) = E^b(\omega)e^{i\omega t} + E^b(-\omega)e^{-i\omega t}$. The shift-current response is characterized by the third-rank tensor $\sigma^{abc}(0;\omega,-\omega)$ as,

$$J^a_{\rm shift}(\omega) = 2\sum_{bc}\sigma^{abc}(0;\omega,-\omega)E^b(\omega)E^c(-\omega). \qquad (2)$$

Centrosymmetric materials have vanishing shift current since the left hand side of Eq. 2 changes sign under inversion but not the right hand side. The shift-current tensor is given by [3]

$$\sigma^{abc}(0;\omega,-\omega) = -\frac{i\pi e^3}{2\hbar^2}\int\frac{d\mathbf{k}}{8\pi^3}\sum_{nm}f_{nm}\big(r^b_{mn}r^c_{nm;a} + r^c_{mn}r^b_{nm;a}\big)\delta(\omega_{mn}-\omega), \qquad (3)$$

where, as in Eq. 1, r^a_{mn} are the dipole matrix elements and the generalized derivatives defined as $r^a_{mn;b} = \partial r^a_{mn}/\partial k^b - i(A^b_{nn} - A^b_{mm})r^a_{nm}$. For linear polarization, $b = c$, and the integrand in Eq. 3 is proportional to the shift "vector" $R^{a,b}_{nm}$ as discussed below.

Fig. 2 shows calculated shift-current spectra for GeS and SnSe parallel and perpendicular to the polarization axis (The shift-current spectra for GeSe and SnS have similar features, see SI.) We find a broad maximum of the order of 200 μA/V^2 which, importantly, occurs in the visible range ($1.5 - 3.3$ eV). The in-plane components, zzz and zyy, are larger than the out-of-plane component zxx, as expected. We can compare this response with predicted or measured photovoltaic effects for prototypical ferroelectic materials in the same frequency range, e.g., 0.1 μA/V^2 in $BiFeO_3$ [5], and 10 μA/V^2 in $BaTiO_3$ [5]. Additionally, 1 μA/V^2 is reported for hybrid halide perovskites [5] and $NaAsSe_2$ [32], and 500 μA/V^2 is measured in state-of-the-art Si-based photovoltaic technology [33]. The large induced shift current demonstrates

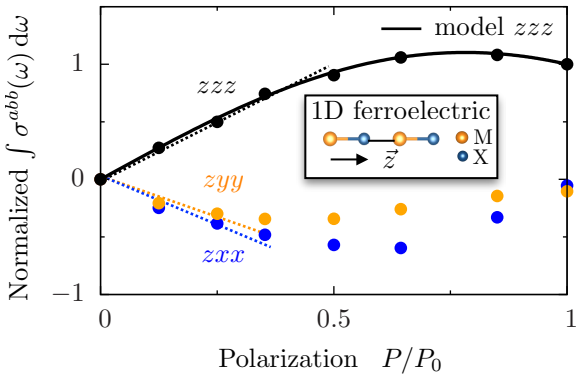

FIG. 3. (Color online) Non-monotonic dependence of the integral of the shift-current tensor vs. electric polarization for GeS; the integral is normalized by -3×10^{10} As^{-1}V^{-2}, its value at the ground state with polarization $P_0 = 1.9$ C/m^2. For small polarizations the integral is directly proportional to polarization, as expected, but it is non-monotonic for large polarization. The inset shows an effective Rice-Mele tight-binding model for the monochalcogenide. We find a good agreement with ab-initio calculations (black line) and the model with parameters $(t,[0,\delta_0],\Delta_0) = (1,[0,-0.865],0.4)$ eV. Physically, the polarization can be modified by applying an electric field or strain.

the potential of monolayer monochalcogenides for optoelectronic applications. The absorption and shift-current spectra are related by the dipole matrix elements $|r_{mm}|^2$ entering Eq. 1 and 3, explaining why peaks in the density of states tend to correspond to peaks in the shift current spectra. Moreover, wavefunction Berry phases contribute additional structure to the shift-current spectra by means of the shift vector in Eq. 3, which we explore next.

Application. To motivate our results, consider an idealized current source illuminated by unpolarized light with a flat and broad spectrum. The short-circuit current in the z-direction, $I_{\rm sc} = AE_0^2\int d\omega(\sigma^{zyy}(0;\omega,-\omega) + \sigma^{zzz}(0;\omega,-\omega))$, is proportional to the integral of the shift current tensor. The cross sectional area is A and the amplitude of the electric field is E_0. We can examine how the integral varies as a function of polarization. To

first non-vanishing order in λ both the polarization and the integral are linear in λ, $P(\lambda) = \partial_\lambda P(0)\ \lambda + \cdots$, $\int \sigma^{abb}(\lambda) = (\int \partial_\lambda \sigma^{abb}(0))\ \lambda + \cdots$, and hence proportional to each other. In Fig. 3 we show the integral of the shift-current tensor over the frequency range (up to 6 eV) for GeS as a function of polarization along the adiabatic path of Fig. 1b. For small polarization, the integral grows linearly with polarization, as expected. However, for larger polarization there is non-monotonic behavior which we explain with a tight-binding model. Notice that without the integral, the expansion coefficients become frequency dependent and the current could increase or decrease with polarization with no general relationship.

The Rice-Mele tight-binding model and shift current. As mentioned previously, the chalcogenide single-layer has a $2[001]+(1/2,0,1/2)$ symmetry that transforms the the upper three atoms in Fig. 1b onto the lower three. This suggests there is an effective one-dimensional description of the armchair structure in the z direction, and in fact, as we show below, the trends in the integral of the shift-current tensor along z is captured by a simple model Rice-Mele (RM) model [34, 35]. The RM Hamiltonian is

$$H = \sum_i \left[(\frac{t}{2} + (-1)^i \frac{\delta}{2})(c_i^\dagger c_{i+1} + h.c.) + (-1)^i \Delta c_i^\dagger c_i \right], \tag{4}$$

where δ parametrizes the distortion relative to the centrosymmetric structure, Δ the staggered on-site potential and $c_i^\dagger$ is the creation operator for electrons at site i. Inversion symmetry is broken when both $\Delta \neq 0$ and $\delta \neq 0$, and preserved otherwise. For this two-band model Eq. 3 gives (see SI for more details),

$$\int d\,\omega\ \sigma^{zzz}(0;\omega,-\omega) = e^3 \int dk\ \frac{|v_{cv}|^2 R_{cv}}{4E^2}, \tag{5}$$

where $R_{cv} = \partial\phi_{cv}/\partial k + A_{cc} - A_{vv}$ is the shift vector and is gauge invariant. $A_{nm} = i\langle u_n|\partial_k|u_m\rangle$ are the Berry connections, and ϕ^b_{nm} is defined by $r^b_{nm} = |r^b_{nm}|e^{-i\phi^b_{nm}}$, where $E(k)$ is the band dispersion and v_{cv} is the matrix element of the velocity operator. The Rice-Mele model allows for a complete analytic solution for many optical responses. These results will be presented elsewhere [36]. The polarization is $P(\delta) = (e/2\pi)\int dk\ (A_{vv}(k,\delta) - A_{vv}(k,0))$ mod e. The model has two independent parameters δ and Δ. $t = 1$ eV gives an overall energy scale, and δ and Δ are related by the energy gap, $2\sqrt{\delta_0^2+\Delta_0^2} = 1.9$ eV. Choosing parameters $(t,[0,\delta_0],\Delta_0) = (1,[0,-0.865],0.4)$ eV fits the zzz ab-initio integral for GeS well and yields a gap 1.9 eV, in close agreement with the gap at the Γ point for GeS. The RM model polarization is $P_0 = P(\delta_0 = -0.865)$. Our results show the RM model is a good description of the integral of the shift-current tensor in monochalcogenides and we now explore the relation between polarization and shift current within this model.

Analysis of Eq. 5 shows that the integral is determined by the competition between the shift vector and the velocity matrix elements $\hbar^2|v_{cv}|^2/4E^2 \equiv |r_{cv}|^2$. These factors are controlled by δ and Δ in our model and have opposing tendencies: whereas increasing Δ localizes the wave function at sites with potential $-\Delta$, increasing dimerization δ moves the valence center of charge away from them. We find that for $\delta \ll \Delta$, R_{cv} is sharply peaked at $k = 0$ but $|v_{cv}|^2/4E^2$ peaks at π/c hence the integral small. As δ increases the peak in R_{cv} and $|v_{cv}|^2/4E^2$ broadens increasing the integral. However, their peak maximum also decreases. In this regime the integral reaches a maximum at an optimum value, $\pm\delta_m$ which to lowest order in Δ is

$$\delta_m = \Delta + O(\Delta^3 \log\Delta), \tag{6}$$

where the polarization takes the value $P(\delta_m)$. For $\delta \gg \Delta$ the matrix elements are momentum-independent but the integral is small and decreasing with increasing δ, as seen in Fig. 3.

Discussion and conclusions We have calculated the shift-current response and spontaneous electric polarization of a family single-layer monochalcogenides: MX where M = Ge, Sn, and X = S, Se. We find a large shift current and a large polarization compared with prototypical ferroelectric materials. The fact the maximum current occurs in the visible range highlights the potential of these materials for optoelectronic applications. Further, the large spontaneous polarization can serve as knob to engineer the photoresponse or conversely a large shift current can induce a large polarization change $\Delta P = \int J_{\rm shift} dt$ which can alter the polarization. While no relation is found between polarization and the shift current at a single frequency, the integral of the shift-current tensor over frequency is well described by the Rice-Mele model and we find an optimal value of polarization where the current is maximum. We believe this behavior is general to other ferroelectrics described by the RM model.

BMF and TR share equal contributions. We thank J. Sipe, F. de Juan, S. Barraza-Lopez, S. Coh, R. A. Muniz, S. E. Reyes-Lillo for useful discussions. BMF acknowledges support from AFOSR MURI, Conacyt and NERSC contract No. DE-AC02-05CH11231. TM acknowledges support from the Gordon and Betty Moore Foundation's EPiQS Initiative Theory Center Grant. JEM acknowledges LDRD funding from LBNL Contract No. DEAC02-05CH11231. BSM acknowledges partial support from CONACYT-Mexico GoGa no. 153930. This work is supported by the U.S. Department of Energy, Director, Office of Science, Office of Basic Energy Sciences, Materials Sciences and Engineering Division, under Contract No. DE-AC02-05CH11231, through the Theory FWP [KC2301] in LBNL. This work is also supported by the Molecular Foundry through the DOE, Office of Basic Energy Sciences under the same contract number.

We acknowledge the use of computational resources at the NERSC.

* These two authors contributed equally.

[1] B. I. Sturman and P. J. Sturman, *Photovoltaic and Photo-refractive Effects in Noncentrosymmetric Materials* (CRC Press, 1992).

[2] R. von Baltz and W. Kraut, Phys. Rev. B **23**, 5590 (1981).

[3] J. E. Sipe and A. I. Shkrebtii, Phys. Rev. B **61**, 5337 (2000).

[4] L. Z. Tan, F. Zheng, S. M. Young, F. Wang, S. Liu, and A. M. Rappe, Npj Comput. Mater. **2**, 16026 (2016).

[5] S. M. Young, F. Zheng, and A. M. Rappe, Phys. Rev. Lett. **109**, 236601 (2012); S. M. Young and A. M. Rappe, *ibid.* **109**, 116601 (2012); F. Zheng, H. Takenaka, F. Wang, N. Z. Koocher, and A. M. Rappe, J. Phys. Chem. Lett. **6**, 31 (2015).

[6] A. Zenkevich, Y. Matveyev, K. Maksimova, R. Gaynutdinov, A. Tolstikhina, and V. Fridkin, Phys. Rev. B **90**, 161409 (2014).

[7] A. M. Cook, B. M. Fregoso, F. de Juan, and J. E. Moore, "Design principles for shift current photovoltaics," ArXiv:1507.08677 [cond-mat.mes-hall].

[8] A. K. Singh and R. G. Hennig, Appl. Phys. Lett. **105**, 042103 (2014).

[9] F. Wang, S. M. Young, F. Zheng, I. Grinberg, and A. M. Rappe, Nat. Commun. **7**, 10419 (2016).

[10] P. Ramasamy, D. Kwak, D.-H. Lim, H.-S. R a, and J.-S. Lee, J. Mater. Chem. C **4**, 479 (2016).

[11] L. Pintilie, I. Vrejoiu, G. L. Rhun, and M. Alexe, J. Appl. Phys. **101**, 064109 (2007).

[12] G. Shi and E. Kioupakis, Nano Lett. **15**, 6926 (2015).

[13] L. C. Gomes, P. E. Trevisanutto, A. S. Carvalho, A. a nd Rodin, and A. H. C. Neto, arXiv:1607.07564 [cond-mat.mes-hall] (2016).

[14] X. Gonze *et al.*, Comput. Phys. Commun. **205** (2016), 10.1016/j.cpc.2016.04.003.

[15] M. Krack, Theor. Chem. Acc. **114**, 145 (2005).

[16] J. P. Perdew, K. Burke, and M. Ernzerhof, Phys. Rev. Lett. **77**, 3865 (1996).

[17] P. N. Butcher, *Nonlinear Optical Phenomena* (Engineering Experiment Station of the Ohio State University, 1965).

[18] D. Vanderbilt and R. D. King-Smith, Phys. Rev. B **48**, 4442 (1993).

[19] R. Resta, J. Phys.: Condens. Matter **22**, 123201 (2010).

[20] M. Mehboudi, B. M. Fregoso, Y. Yang, W. Zhu, A. van der Zande, J. Ferrer, L. Bellaiche, P. Kumar, and S. Barraza-Lopez, "Structural phase transition and material properties of few-layer monochalcogenides," ArXiv:1603.03748 [cond-mat.mtrl-sci].

[21] R. Fei, W. Kang, and L. Yang, "Robust ferroelectricity in monolayer group-iv monochalcogenides," ArXiv:1604.00724 [cond-mat.mtrl-sci].

[22] L. C. Gomes, A. Carvalho, and A. H. Castro Neto, Phys. Rev. B **92**, 214103 (2015).

[23] R. Fei, W. Li, J. Li, and L. Yang, Applied Physics Letters **107**, 173104 (2015).

[24] H. Wang and X. Qian, "Two-dimensional multiferroics: Ferroelasticity, ferroelectricity, domain wall, and potential mechano-opto-electronic applications," ArXiv:1606.04522 [cond-mat.mtrl-sci].

[25] R. Fei, W. Kang, and L. Yang, Phys. Rev. Lett. **117**, 097601 (2016).

[26] R. D. Johnson, L. C. Chapon, D. D. Khalyavin, P. Manuel, P. G. Radaelli, and C. Martin, Phys. Rev. Lett. **108**, 067201 (2012).

[27] A. von Hippel, Rev. Mod. Phys. **22**, 221 (1950).

[28] J. Shieh, J. Yeh, Y. Shu, and J. Yen, Materials Science and Engineering: B **161**, 50 (2009).

[29] R. Resta, M. Posternak, and A. Baldereschi, Phys. Rev. Lett. **70**, 1010 (1993).

[30] J. B. Neaton, C. Ederer, U. V. Waghmare, N. A. Spaldin, and K. M. Rabe, Phys. Rev. B **71**, 014113 (2005).

[31] G. Catalan and J. F. Scott, Advanced Materials **21**, 2463 (2009).

[32] J. A. Brehm, S. M. Young, F. Zheng, and A. M. Rappe, The Journal of Chemical Physics **141**, 204704 (2014).

[33] M. Pagliaro, G. Palmisano, and R. Ciriminna, *Flexible Solar Cells* (Wiley-VCH; 1 edition, 2008).

[34] D. Vanderbilt and R. D. King-Smith, Phys. Rev. B **48**, 4442 (1993).

[35] S. Onoda, S. Murakami, and N. Nagaosa, Phys. Rev. Lett. **93**, 167602 (2004).

[36] B. M. Fregoso *et al.*, To be published.

[37] The ABINIT web site: `http://www.abinit.org`.

Supplementary information: Giant bulk photovoltaic effect and electric polarization of single-layer monochalcogenides

In this Supplementary Information we present details of our electric polarization and shift current calculation for GeS, GeSe, SnS and SnSe. We also provide details of the shift current and polarization in the Rice-Mele model.

Numerical details

Our density functional theory (DFT) calculations are done with the ABINIT code [14] and within the Perdew-Burke-Ernzerhof functional (PBE) [16]. We use Hartwigsen-Goedecker-Hutter norm conserving pseudopotentials available in the ABINIT web site [37]. We use an energy cut-off of 40 hartrees to expand the plane-wave basis set. To model the slabs we use supercells with 15 Å along the non-periodic direction, which corresponds to $>$ 10 Å of vacuum. To calculate σ we include 20 valence and 30 conduction bands, which accounts for all allowed transitions in the low energy range; up to 6 eV; we use a mesh of 70×70 k-points along the periodic slab directions and integrate using a tetrahedron method. Worth mentioning that the optical-response and spontaneous-polarization magnitude depend on the calculation volume, therefore we renormalize our results to the atomic slab widths (removing the vacuum) of 2.56, 2.61, 2.84 and 2.73 Å for GeS, GeSe, SnS and SnSe respectively. String method calculations were done with the ABINIT code as explained in Sect. 3.2 of Ref. 14, where the minimal energy path between two points was found using 50 images and a tolerance on the mean total energy for images of 2×10^{-6} hartrees. In the next, we provide more details on our calculations of spontaneous polarization, the ferroelectric energy barrier and optical responses of the monochalcogenides.

Spontaneous Polarization

We calculate the spontaneous polarization as implemented in ABINIT using

$$P^a(\lambda) = \sum_i \frac{eZ^i r_i^a(\lambda)}{\Omega} - \mathrm{i}e \sum_v \int_{\mathrm{BZ}} \frac{d\mathbf{k}}{(2\pi)^3} \langle u_v^\lambda | \nabla^a u_v^\lambda \rangle, \quad (7)$$

where u_v^λ are Bloch wave functions, Z^i is the atomic number of the ith atom, Ω is the simulation volume. λ parametrizes an adiabatic path from a centrosymmetric configuration to the ground-state configuration. The polarization is defined as the difference between the polarization of two smoothly connected atomic structures: $\mathbf{R}_0^i$ with inversion symmetry (i.e., zero of polarization) and $\mathbf{R}_f^i(\lambda = 1)$, where $\mathbf{R}_f^i = \mathbf{R}_0^i + \lambda(\mathbf{R}_f^i - \mathbf{R}_0^i)$. The geometry of the $\mathbf{R}_f^i$ and $\mathbf{R}_0^i$ points used in this work are shown in Table II. The polarization calculated at small steps of λ for the different crystals is shown in Fig. 4. Since all points are connected smoothly, the polarization is well-defined and can be calculated as the difference between the polarization at $\mathbf{R}_0^i$ and $\mathbf{R}_f^i$. The resulting spontaneous polarization values of the different crystals are tabulated in Table. 1 of the main manuscript.

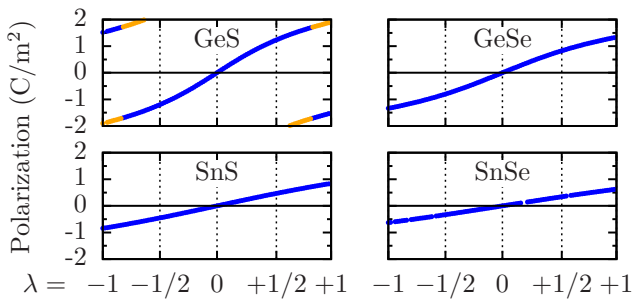

FIG. 4. Polarization along adiabatic path parametrized by λ. The gap does not closes along the path and takes the system from polarization $-P_0$ ($\lambda = -1$) to 0 ($\lambda = 0$) to $+P_0$ ($\lambda = +1$). The calculated polarization (blue dots) is shifted by the twice polarization quantum ($Q = 1.7$ C/m^2) for GeS (orange dots).

Minimum energy path

Here we detail how we evaluate the ferroelectric energy barrier between the two ground-states with inverse polarization $\pm P_0$. We first calculate a path of fifty equidistant-potential points connecting the two frontier points using the string method. Note that with this grid of points we cannot evaluate the polarity of the central point due to numerical remaining errors. Hence, to obtain the precise coordinates of the saddle point, for GeS we calculate a finer grid of thirty equidistant-potential points in between the two central points of the fifty-point initial path. In Fig. 5 we show the energy barrier and initial, central and final configurations along the trajectory for GeS. The resulting coordinates of the highest-energy saddle point (Fig. 5b) are

Atom coordinates (Å):

Ge	1.54	0.91	0.00
Ge	3.84	2.74	2.24
S	3.86	0.91	0.00
S	1.51	2.74	2.24

which resemble those of the ideal R_0 point (see Fig.1 of the main text and coordinates in Table II); while the x Cartesian component is slightly modified by ~ 0.1 bohr, the y and z Cartesian components are identical, implying zero-polarization along z. In terms of energetics, the

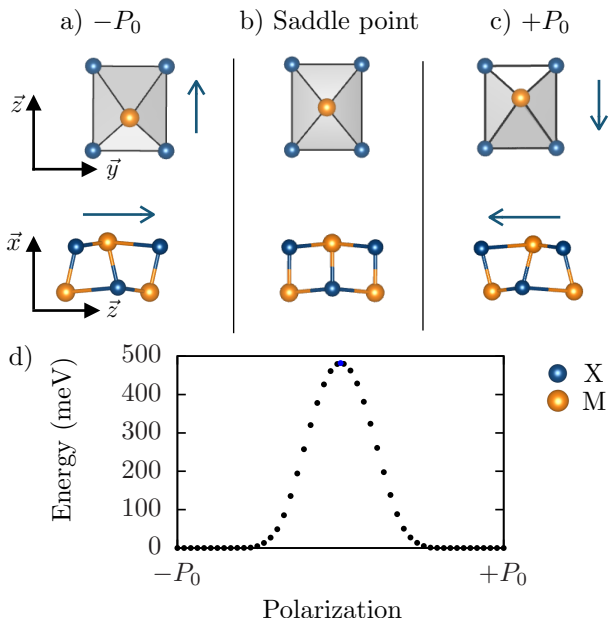

FIG. 5. Ferroelectric energy barrier of GeS calculated using the string method. Insets a-c: ground state configurations with polarization $\pm P_0$ and saddle point. Inset d shows the calculated energy barrier, with the saddle point in blue.

saddle-point total energy is ~ 70 meV lower than that of the R_0 point.

Electronic bandstructures

The electronic bandstructures calculated within DFT are shown in Fig. 8, these agree with previous works [8]. For each material the fundamental gap E_g is indicated in the figure with an arrow.

Shift current responses

We noticed that shift-current responses converge relatively slow with respect to the number of k-points. As shown in Fig. 6, for GeS we require a dense mesh of 70×70 k-points on the slab plane to converge, removing sudden jumps (e.g., see blue and pink lines close 2.5 eV) in the response.

In Fig. 7, we show our calculated linear and shift-current responses of the layered monochalcogenide materials studied in this work. As mentioned in the main text, the responses are higher along zzz and zyy directions than for zxx and are relatively large.

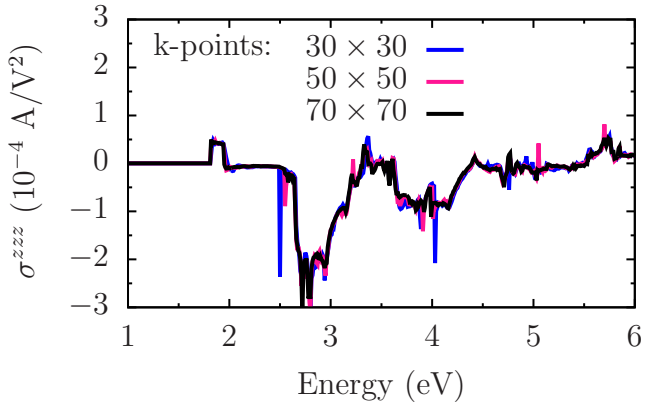

FIG. 6. Convergence of shift-current tensor for GeS with respect to the **k**-mesh size.

Shift current and polarization in the Rice-Mele model

In this section we provide some details of the derivation of the shift current for the one dimensional (1D) Rice-Mele (RM) model. Starting from Eq. 3 in the main text we set $b = c$ (linear polarization) and using $r^b_{nm} = |r^b_{nm}|e^{-i\phi^b_{nm}}$ and $r^a_{mn;b} = \partial r^a_{mn}/\partial k^b - i(A^b_{nn} - A^b_{mm})r^a_{nm}$, Eq. 3 takes the familiar form

$$\sigma^{abb}(0;\omega,-\omega) = -\frac{\pi e^3}{\hbar^2}\int \frac{d^dk}{(2\pi)^d}\sum_{nm} f_{nm}|r^b_{nm}|^2 R^{a,b}_{nm}, \tag{8}$$

in terms of the shift shift vector is $R^{a,b}_{nm} = \partial\phi^b_{nm}/\partial k^a + A^a_{nn} - A^a_{mm}$. For a two-band model in 1D, n, m take two values c, v, and hence we obtain Eq. 6 of the main text. In the derivation we used $r^a_{nm} = \langle u_n|v^a|u_m\rangle/i\omega_{nm}$ that is valid for non-degenerate bands. Now we apply this results to the RM Hamiltonian Eq. 4. where δ parametrizes the dimerization of the chain and Δ the staggered on-site potential. Inversion symmetry is preserved when $\delta \neq 0$ and $\Delta \neq 0$ and broken otherwise. The unit cell along z-(of length c) has two sites. Since we are interested in a model with the minimal number of parameters that captures the physics of the monochalcogenides, we set the distance between atoms to be the same and modulate only the hopping. We obtain $\hat{H} = \sum_k (c^\dagger_{k,A}\ c^\dagger_{k,B})H(k)(c_{k,A}\ c_{k,B})^T$ with Bloch Hamiltonian,

$$H = \sigma_x\ t\cos(ka/2) - \sigma_y\ \delta\sin(ka/2) + \sigma_z\ \Delta \tag{9}$$

and cell periodic functions u_n such that $Hu_{c,v} = \pm Eu_{c,v}$. The eigenvalues are given by $E = \sqrt{t^2\cos^2 ka/2 + \delta^2\sin^2 ka/2 + \Delta^2}$ for the conduction and $-E$ for the valence bands. Berry connections will depend explicitly on the gauge used but the results on

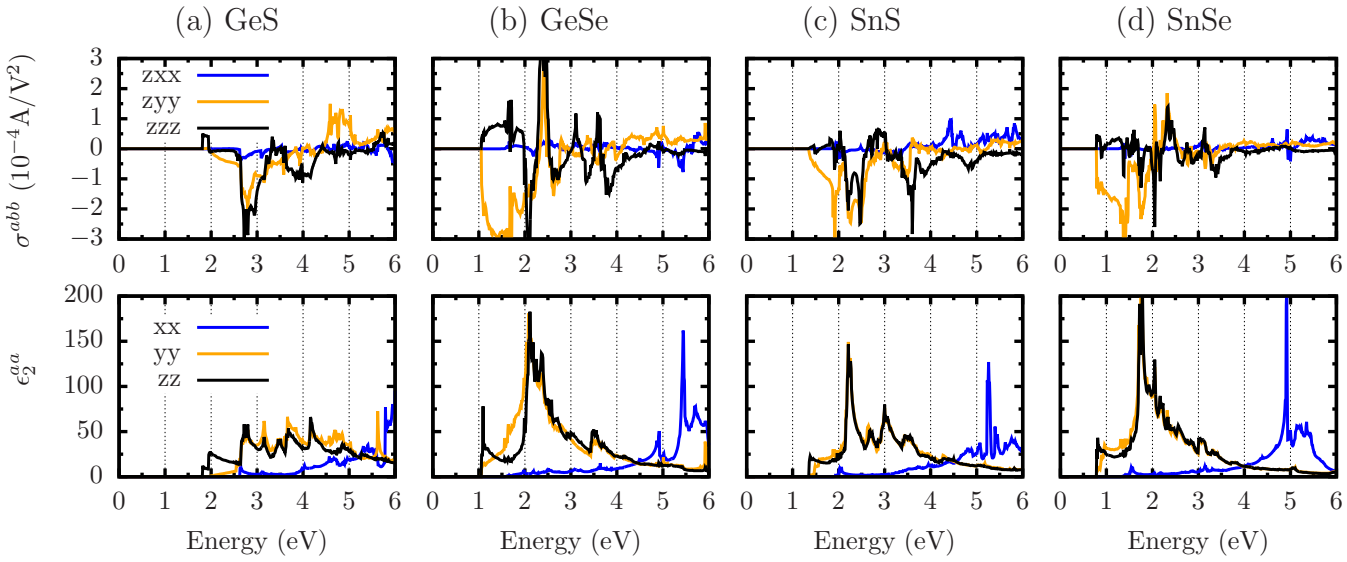

FIG. 7. Shift current (top) and linear response (bottom) of monolayer monochalcogenides. The large shift current and linear absorption ($\epsilon_2 \sim 100$) induced in the visible range of frequencies indicate their positive potential for optoelectronic applications.

the shift vector and shift current are gauge independent. We then compute the shift current and polarization from the Berry connections and velocity matrix elements. If the electric field is along the chain, the z-direction, the shift current is

$$J^z_{\rm shift}(\omega) = 2\sigma^{zzz}(0;\omega,-\omega)E^z(\omega)E^z(-\omega). \qquad (10)$$

For the two-band model

$$\sigma^{zzz} = e^3 \int_0^{2\pi/a} dk \; \frac{|\langle u_c|v|u_v\rangle|^2 R_{cv}}{\hbar^2\omega^2}\delta(\frac{2E}{\hbar}-\omega) \qquad (11)$$

To quantify the amount of shift current generated in short-circuit mode we define the 'average conductivity tensor' as,

$$\int d\omega \; \sigma^{zzz}(0;\omega,-\omega) = e^3 \int dk \frac{|\langle u_c|v|u_v\rangle|^2 R_{cv}}{4E^2} \qquad (12)$$

This integral is shown in the main text. It can be expressed analytically in terms of elliptic functions [36]. Here chose model parameters $(t,[0,\delta_0],\Delta_0) = (1,[0,-.865],.4)$ eV that fit the ab-initio shift current data for GeS. In Fig. 3 in the main text we normalized the vertical and horizontal axis with respect to the results at the ground state $(t,\delta_0,\Delta_0) = (1,-.865,.4)$.

TABLE II: Geometry (in Å) of single-layer monochalcogenides used to compute the spontaneous polarization along an adiabatic path connecting $\mathbf{R}^i_f(\lambda=-1)$ to $\mathbf{R}^i_f(\lambda=1)$, read manuscript.

GeS
Lattice parameters:
$\vec{a}=$ 15.00 0.00 0.00
$\vec{b}=$ 0.00 3.66 0.00
$\vec{c}=$ 0.00 0.00 4.47
Atom coordinates:

	R_0			$R_f(\lambda=1.0)$			$R_f(\lambda=-1.0)$		
Ge	1.41	0.91	0.00	1.41	0.91	0.59	1.41	0.91	-0.59
Ge	3.97	2.74	2.24	3.97	2.74	2.83	3.97	2.74	1.64
S	3.76	0.91	0.00	3.76	0.91	0.00	3.76	0.91	0.00
S	1.62	2.74	2.24	1.62	2.74	2.24	1.62	2.74	2.24

GeSe
$\vec{a}=$ 15.00 0.00 0.00
$\vec{b}=$ 0.00 3.98 0.00
$\vec{c}=$ 0.00 0.00 4.26
Atom coordinates:

	R_0			$R_f(\lambda=1.0)$			$R_f(\lambda=-1.0)$		
Ge	1.58	0.99	0.00	1.58	0.99	0.44	1.58	0.99	-0.44
Ge	4.00	2.98	2.13	4.00	2.98	2.58	4.00	2.98	1.68
Se	4.10	0.99	0.00	4.10	0.99	0.09	4.10	0.99	-0.09
Se	1.49	2.98	2.13	1.49	2.98	2.22	1.49	2.98	2.04

SnS
Lattice parameters:
$\vec{a}=$ 15.00 0.00 0.00
$\vec{b}=$ 0.00 4.11 0.00
$\vec{c}=$ 0.00 0.00 4.27
Atom coordinates:

	R_0			$R_f(\lambda=1.0)$			$R_f(\lambda=-1.0)$		
Sn	1.45	1.03	0.00	1.45	1.03	0.47	1.45	1.03	-0.47
Sn	4.29	3.08	2.13	4.29	3.08	2.61	4.29	3.08	1.66
S	4.04	1.03	0.00	4.04	1.03	0.19	4.04	1.03	-0.19
S	1.71	3.08	2.13	1.71	3.08	2.32	1.71	3.08	1.94

SnSe
Lattice parameters:
$\vec{a}=$ 15.00 0.00 0.00
$\vec{b}=$ 0.000 4.31 0.00
$\vec{c}=$ 0.000 0.00 4.38
Atom coordinates:

	R_0			$R_f(\lambda=1.0)$			$R_f(\lambda=-1.0)$		
Sn	1.58	1.08	0.00	1.58	1.08	0.41	1.58	1.08	-0.41
Sn	4.33	3.23	2.19	4.33	3.23	2.60	4.33	3.23	1.78
Se	4.31	1.08	0.00	4.31	1.08	0.22	4.31	1.08	-0.22

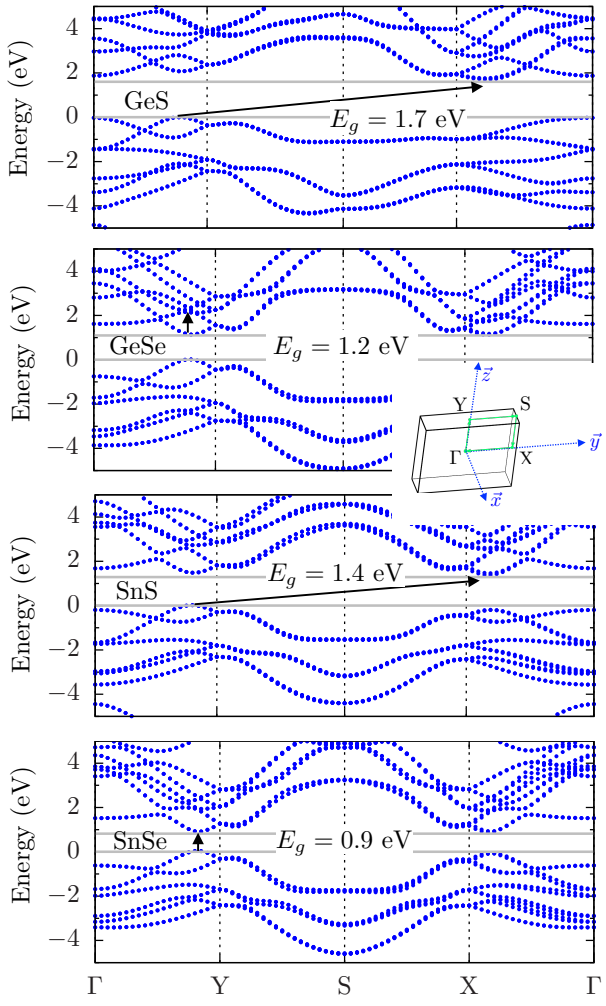

FIG. 8. Electronic bandstructure of group-IV single-layer monochalcogenides, calculated within DFT-PBE. We choose a k-point path along the Brillouin zone, shown at the bottom.

Se	1.61	3.23	2.19	1.61	3.23	2.41	1.61	3.23	1.97